Conformable transducers for large-volume, operator-independent imaging

Chris M.W. Daft
Siemens Ultrasound, Mountain View, CA, USA
daft@ieee.org

***Abstract*—While ultrasound's cost, safety and interesting contrast mechanisms are of great clinical value, its operator-dependence, extensive sonographer training needs, uncompetitive scan times, poor ergonomics and low reproducibility in serial studies limit its proliferation. This paper examines opportunities to solve these problems and increase ultrasound's application space via arrays which conform to the patient's body contours. Progress towards a conformable array maintaining ultrasound's existing feature set has been promising, but a complete system is yet to be demonstrated. The article first outlines the motivation for such arrays, defines design requirements, and describes an ideal design. Next, work on partial hardware realizations of conformable arrays is reviewed, and types of signal processing specific to conformable systems are discussed. Finally, future research directions are envisioned.**

Operator-independent ultrasound requires large acquisition volumes with voxels isotropic enough to allow post-scan clinical assessment without regard for scanning geometry. *Information rate* is presented as a useful metric to compare the diagnostic utility of these systems. Two new hardware realizations are described to illustrate progress towards the conformable array goal. An automated breast-scanning design with a matrix receiver using silicon transducers (cMUTs) shows provocative performance in a micro-calcification detection simulation. A reconfigurable matrix array, also using cMUTs, provides volume imaging performance characteristic of a fully-sampled aperture with sufficiently modest interconnect demands to be feasible in a transesophageal echo (TEE) application.

Keywords: *medical ultrasound; 3D; silicon transducer, cMUT; MEMS; capacitive micromachined transducer; volume imaging, breast screening, conformable array, flexible probe.*

I. INTRODUCTION

The clinical utility of ultrasound is currently defined by a balance between strong positive and negative factors. Its relatively low cost, safety, ability to image tissue movement and stiffness, and lack of ionizing radiation are undeniable strengths. But ultrasound's operator-dependence, extensive sonographer training requirements, increasingly uncompetitive scan times relative to CT and MR, poor ergonomics and low reproducibility in serial studies have been noted as severe defects [1].

This paper examines ways to deal with these problems and increase medical ultrasound's applicability by developing transducers which conform to the contours of the patient's body. Progress towards such a conformable array has been promising, but a complete transducer has not yet been demonstrated. This article therefore combines a review of prior published work, a description of requirements for a complete device, an approach to evaluating designs, two new developments, and speculation on future research directions.

Attempts at operator-independent scanning began a number of years ago with DARPA-funded research without flexible arrays. Since then, certain commercial products have secured clinical advantages which are examined. Then we consider what a fully expressed conformable array reaching the goals of large volume, operator-independent acquisition would look like. For example, clinical requirements presuppose voxels isotropic enough that the eventual (possibly off-site) reading of the scan will be valid regardless of the scan orientation. Some consequences of these requirements are worked through. *Information rate* is a useful metric to compare the diagnostic utility of differing approaches.

Next, research from several groups which constitutes significant steps towards this kind of scanning is reviewed. These results are grouped into hardware and signal-processing sections; while the need for new kinds of hardware is obvious, there will also be much unique signal processing in any successful conformable array system.

The partial realizations discussed include flexible transducers with a variety of constructions, probe-moving systems that collect data in a more operator-independent fashion, and reconfigurable arrays. Signal processing for a conformable array requires location of the transducer element positions and orientations; compensation for elements blocked by, e.g., bone; means to achieve adequate acquisition speed; registration and stitching of overlapping volumes, and phase aberration correction. Finally, an assessment is given of the gaps between what has been developed and what would be needed for a full system.

This paper uses the term *conformable* rather than *conformal* in describing a flexible array, even though *conformal* is more usual in the literature for this type of transducer. *Conformal* has significantly different meanings in several fields of mathematics, as well as in cartography and physics, although in describing coatings in electronics manufacturing *conformal* takes the meaning intended here. It appears that *conformable* can only be confused with a property of matrices in linear algebra, so using that word may propagate less misunderstanding.

II. EARLY OPERATOR-INDEPENDENT SCANNING

Before examining conformable solutions, it is worth considering non-conformable approaches to the problem of operator-dependence in ultrasound. Progress began when

DARPA funded a project called MUSTPAC (Medical Ultrasound, Three-dimensional, Portable, with Advanced Communications, [2]). This was a 3D telemedicine system in which an untrained operator performed a large-volume acquisition with a traditional 1D slice probe. To acquire 3D data, the operator used either a motor-driven probe mover or freehand motion orthogonal to the scan plane. A remote clinician interpreted the data transmitted to their location later, with confidence the correct data would be contained somewhere within the large anatomical volume scanned. A "virtual probe" interface was developed to improve the reviewing clinician's workflow. The MUSTPAC equipment was tested in a variety of hostile environments, including an expedition to Mt. Everest. While the work had a telemedicine rather than an ultrasound emphasis, it showed that a combination of 3D data acquisition by an untrained operator plus remote clinician interpretation works in a variety of scenarios. It was no surprise that 3D data was essential for results with any clinical value.

This early project lacked Doppler functions; there was no representation of anatomic motion to the clinician, and it exhibited sensitivity to shadowing effects which could not be compensated for by expertly moving the transducer. It also suffered from the imager parameters not being set by a trained sonographer. However, there has been a great deal of progress on automated parameter adjustment in commercial systems since the MUSTPAC project's conclusion in 2000.

More recently, two commercial imagers have made progress towards operator-independent scanning of the entire breast. These contain long (~15 cm) slice-acquiring transducers which are moved orthogonally to the scan direction. The workflow goal of these products was to allow an X-ray technician with little ultrasound experience to swiftly perform a supplementary ultrasound scan to create diagnostic confidence after an equivocal mammogram.

Regardless of the means of acquisition or any potential workflow improvements, large ultrasound volumes have immediate clinical advantages which have been summarized in, e.g., [3]. Physicians with experience in areas other than ultrasound can better understand anatomic relationships given a larger context and the ability to slice the volume arbitrarily. Size, volume and distance measurements among large organs become possible. And visualizing structures from a variety of angles, where the acoustic windows permit, yields new and valuable information.

III. Defining Design Requirements

A. Physical and electronic requirements

Figure 1 indicates how a flexible array formed from a number of acoustic tiles contacts the body. For successful imaging, the array must be flexible enough for reliable acoustic contact to be achieved over its entire surface area. This is straightforward if the tiles are reasonably small; a more strenuous requirement is the obvious need to acquire a continuous volume over all depths, including at the skin line. Achieving this requires an acoustically transparent layer interposed between the tiles and the skin.

If we consider an array made of rigid tiles embedded in some flexible fabric, whose acoustic construction allows for steering to an angle θ_{MAX} in azimuth and φ_{MAX} in elevation, a simple calculation shows that the gaps Δx and Δy between the tiles must not exceed $\Delta x = 2w \cdot \tan\theta_{MAX}$ or $\Delta y = 2w \cdot \tan \varphi_{MAX}$, respectively, where w is the thickness of the layer.

Other basic requirements include:

- A diagnostically useful center frequency and bandwidth.
- Low enough electronic power dissipation to meet surface temperature requirements (e.g., IEC 60601).
- Low enough acoustic output to conform to Mechanical Index (MI) and Thermal Index (TI) regulatory limits.
- Feasible interconnect, given a large element count ($>10^5$) and the requirement for adequate flexibility.

B. Data integrity

Data integrity for a conformable array has several components. Adequate overlap of acquisitions from several tiles is critical. To achieve operator independence, corrupted final volumes created by shadowing or occlusion must be very rare, and the system must detect this condition, as well as the situation where significant portions of the tissue volume are not being scanned from tiles positioned at more than one angle.

A system capable of larger steering angles and/or smaller gaps Δx and Δy will always be advantageous since greater data redundancy can be obtained. The "straight ahead" volume acquired by a tile of dimensions x and y is $V_S = xyz$ where z is the maximum scan depth; but as Figure 2 shows, there are four rectangular prisms (orange) and four trirectangular tetrahedral volumes (green) accessible by steering. Together, these offer a redundant scan volume which, when Δx and Δy are small compared with $z \cdot \tan \theta_{MAX}$ and $z \cdot \tan \varphi_{MAX}$, can approach:

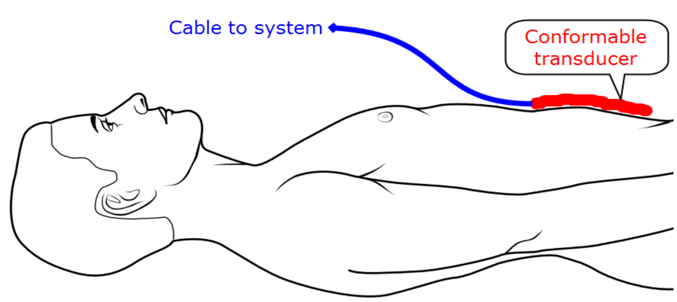

Figure 1: A flexible conformable transducer is placed in acoustic contact with the patient using coupling gel. It deforms to the contours of the body and acquires volume data without need for manipulation during scanning.

$$V_R = \frac{1}{2} yz^2 \tan\theta_{MAX} + \frac{1}{2} xz^2 \tan\phi_{MAX} + \frac{2}{3} z^3 \tan\theta_{MAX} \tan\phi_{MAX}$$

where the first two terms are from the rectangular prisms, the third is from the rectangular tetrahedra, and the coupling layer has been ignored to simplify the geometry.

Such overlapping acquisition makes the stitching of data from several tiles numerically less ill-posed, and also offers speckle reduction without loss of resolution *via* spatial compounding. These topics are covered in more detail later. Besides this, three other data integrity concerns are:

- Low enough motion sensitivity. Motion tracking is possible, but greatly increases the computational burden of scanning. If this is ruled out, the total *coherent* acquisition time cannot exceed around 100 ms in, e.g., abdominal imaging. This becomes critical when synthetic aperture schemes are used. Incoherent acquisition times, for compounding or SNR improvement, can be somewhat longer.
- Low enough sidelobe energy. This means the co-array or effective aperture [4], pp. 454-455 cannot fall to zero or suffer a discontinuity within its region of support in *k*-space.
- Low enough aberration sensitivity. While synthetic aperture approaches can create high-quality volume data in phantoms with only four transmit events, tissue inhomogeneities demand redundant firings over the same volume in order to make the image reconstruction robust.

C. Acquisition capacity

Acquisition capacity drives most of the signal-processing design in a conformable array. Put simply, the acquisition time must be short enough to compare favorably to modalities such as CT and MR, which have from their beginnings imaged large volumes with little operator-dependence.

A convenient way to analyze this requirement is to consider the *information rate* of the system [5]. This is the product of the volume acquired and the information density divided by the voxel volume. The information density is the product of the number of statistically independent voxels in unit volume

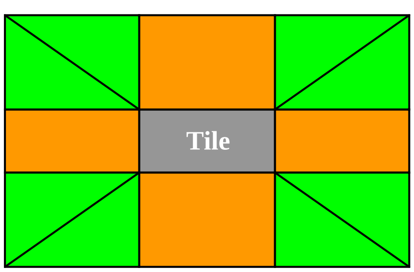

Figure 2: Plan view of "straight-ahead" scan volume (gray) and steering volumes (orange and green). Note that the steered volumes can easily exceed the straight-ahead volume for attainable steering angles

and the square of the contrast-to-noise ratio.

This definition is invariant to simple ways of increasing scan speed such as enlarging the line spacing. These do not affect the information-gathering process key to the diagnostic value of ultrasound. It also acknowledges that there are techniques such as incoherent compounding which do not improve point resolution, but do increase the information retrieved from the tissue by increasing the ratio of mean intensity to fully-developed speckle standard deviation.

D. System demands

Large-aperture conformable arrays can easily create a data rate which overwhelms today's imaging systems. A typical 1D probe might create pre-beamformer data with 12 bits of resolution, digitized at 40 MHz, over 128 channels. This data stream exceeds 60 Gbits/s and can increase by 2-4 orders of magnitude as we move to a matrix probe. Radical means of reducing this data rate are required to make a conformable array practical. Two possibilities considered here are beam formation at the transducer element (section V.B) and reconfigurable chains of elements (section V.C).

E. Unique signal processing needs

While ultrasound machines already contain a variety of post-beamformer signal-processing techniques for image formation, edge enhancement and parameter estimation (particularly for blood flow and elastography) a conformable array needs several types of signal processing not typically found in commercial products:

- The element locations must be determined before scanning can start.
- Blocked elements are always present, and their effects cannot be side-stepped by having a skilled sonographer reorient the transducer.
- Registration and combination of overlapping volumes from each tile are required.
- Very high data rates are necessary. This is due to the increased volume size, and the number of beams which fit in that volume.
- Aberration correction is highly desirable to increase the achievable aperture size and the robustness of the volume reconstruction.

IV. Idealized Conformable Transducer Design

A. Layout

In this section an ideal conformable array is described, to provide additional context and to show the relevance of the partial realizations reviewed in section V. Figure 3 shows a side view of a hypothetical device with overlapping scans.

In this array, a flexible substrate contains interconnect allowing transducer tiles to communicate with an imaging system. Each tile is attached to the substrate and

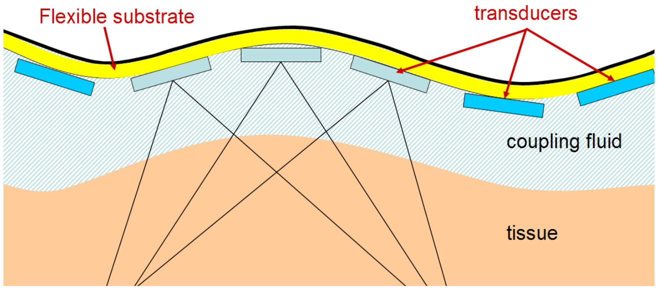

Figure 3: Side view of a conformable array. The transducer tiles are shown mounted on a flexible substrate above a coupling fluid layer. The scanned volumes largely overlap at the skin line to create views from different angles.

incorporates many acoustic elements, but is small enough that the complete device's flexibility allows for reliable acoustic contact through gel. Between the tile and the patient a coupling layer permits overlapping volumes at the skin line. This layer is acoustically transparent, and also provides biocompatibility and conformance to regulatory high-voltage test requirements. Figure 4 is a plan view showing how the tiles fill most of the area of the substrate, while the unfilled margins enhance the flexibility of the device. Could the acoustic tiles themselves be flexible? Capacitive Micromachined Ultrasound Transducers [6] can be made very thin, since their vertical extent is independent of sound wavelength, unlike in piezoelectric transducers. Flexible cMUTs [7] have been made for curved arrays [8] and the same approach could work here.

B. Design Inputs ("Xs") and Outputs ("Ys")

To evaluate practical realizations of this concept, it is helpful to use a Design For Six-Sigma (DFSS) schema as discussed in, e.g., [9]. In this framework, the design parameters we can control are termed *Xs* while the performance relevant to the end-user is quantified as a set of *Ys*. Design consists of finding a functional relationship between these two vectors $\boldsymbol{Y} = \boldsymbol{f(X)}$. Values of the elements of $\boldsymbol{Y}$ show the design's performance, while derivatives $\Delta_{ij} = \partial Y_i / \partial X_j$ quantify the robustness of the design. The X_i become random variables in simulation so that Monte-Carlo or Designed Experiment analysis can show whether achievable control of each X_i will result in small enough variability in performance, as defined by the Y_i. For example, a measure of the contrast achieved by the transducer on an oblique border would be a Y, whereas parameters of a compounding scheme (e.g., [4], pp. 420-421) to improve this Y would be expressed as several X_i. Table 1 lists some of these parameters for a conformable transducer. With this "scratch" design in mind, we turn to a review of real hardware that goes some way towards creating it.

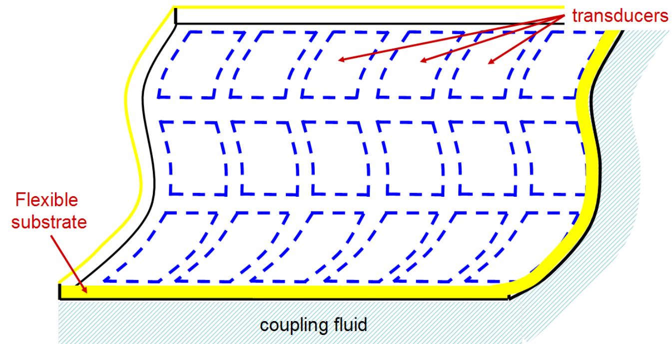

Figure 4: Plan view of conformable array showing an arrangement of tiles with margins between them to create flexibility.

Table 1: DFSS Xs and Ys for a conformable transducer

***Xs*: Controllable design inputs**	***Ys*: Characteristics visible to the user**
Bandwidth and number of interconnects from the tiles to the system	Overall information rate [5] which encompasses imaging voxel size, sidelobe energy and volume rate
Dynamic range and SNR of element plus its electronics	Sensitivity to tissue aberrations
Extent of overlap of scans from neighboring tiles	Maximum volume which can be acquired
Pitch of elements	Field of view at a given depth
Redundancy of imaging scheme	Minimum radius of curvature of transducer
Size of tiles and margin between them	Flow measurement sensitivity
Maximum coherent and incoherent aperture sizes	Degree of operator skill required
Center frequency and bandwidth	Reproducibility from one acquisition to the next
Coupling layer thickness	
Power consumption	

V. REVIEW OF PARTIAL HARDWARE REALIZATIONS

A. Flexible transducers

A UCLA/UCSB collaboration [10] continued MUSTPAC's battlefield application by developing flexible arrays for fracture detection in extremities, as well as evaluation of shrapnel and wound tracts. Figure 5 shows a 12-mm diameter ring-annual array built from PZT elements mounted on top of an array of islands formed from a silicon wafer by Deep Reactive-Ion Etching (DRIE). Polyimide was deposited to form bendable joints, which withstood 10,000 bending cycles to an angle of 60 degrees.

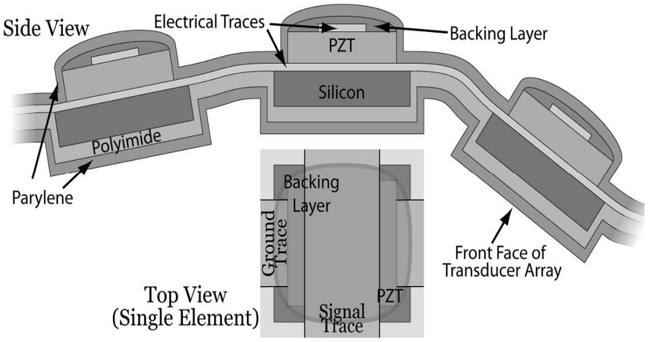

Figure 5: A flexible array design in which each PZT element is separated by flexible polyimide joints (courtesy of A. Dann, UCLA.)

In [11] this group described low-stiffness joints which allow an array to be curved around an index finger, while [12] evaluated an array mounted on copper-cladded polyimide flex with a ground plane on the bottom side. PZT elements were wire-bonded to this flex-circuit with glass and parylene deposited on the top and bottom.

For NDE, Strathclyde University researchers [13] used a single, large transmitter made of modified lead ceramic (MPT) and 64 PVDF receivers. They were able to image pipes with a 100 mm radius of curvature. The transmit element was split into "platelets" to make the array flexible. Figure 6 shows flexible cMUTs made at Stanford University [14] where elements are electrically connected to flip-chip bond-pads on their back side to enable flip-chip connection. The transducers are made flexible by etching 8-50 µm through-wafer trenches and filling them with polydimethylsiloxane (PDMS). They achieved a 0.65 mm radius of curvature, which is small enough to build a side-looking intravascular (IVUS) array. After the cavities are defined, the wafer was fusion-bonded to an SOI blank wafer at 1100°C for an hour. The handle wafer beneath the buried oxide was removed to leave only the silicon above the BOX as the cMUT membrane. The finished devices were robust enough to be handled like regular wafers. Since it is straightforward to integrate these MEMS transducers with electronics [6], such arrays hold considerable promise.

B. Probe-mover systems

Probe-mover systems have been used since the pioneering work of Kirbach [15], but devices pertinent to the current article do not include standard "wobblers," but rather those which make progress in size of volume acquired, and/or operator dependence. Siemens' product known as ABVS (Automated Breast Volume System) is aimed at clinical situations where expert scanning skill is not available. Its use-case involves little user interaction beyond positioning the probe-mover on the breast and starting the acquisition. We have previously [16] described our method to implement the receiver front-end, A/D conversion and beam formation under a 2D cMUT element. This approach works well in a new ABVS design shown in Figure 7, where a 1D array is used for the transmit function, while the receiver is a matrix transducer such as would be required for a fully conformable array. An advantage of the 1D transmitter lies in its utilization of the circuitry within the ultrasound system, which is capable of high power output and arbitrary transmit waveforms for pulse compression and strain imaging. In the new arrangement the existing mechanical translation is retained, but a matrix receiver is introduced with a much larger elevation aperture.

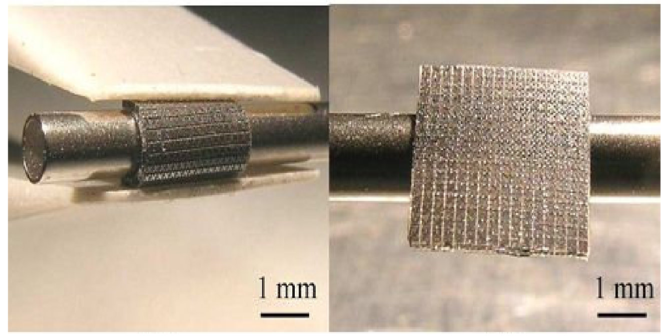

Figure 6: Capacitive (cMUT) array with flexible silicon substrate realized by refilling through-wafer trenches with PDMS (courtesy of P. Khuri-Yakub, Stanford University.)

A PZT transducer could be used for the transmit function, but the continuous elevation receive aperture would be lost since the cMUT receiver matrix would be interrupted. To evaluate the imaging effect of this choice, the simulations of Figure 8 were carried out.

The simulated target is a ring of spherical scatterers with diameter 0.7λ embedded in a speckle phantom. The top row (marked 1) simulates these micro-calcifications, while the lower row (marked 2) includes a coherently scattering tube to mimic a clinical situation such as invasive ductal carcinoma, where the small structures we must detect often appear along the duct walls [17]. In the 1D transducer cases *A1* and *A2* we arranged for the scatterers to be at the focus of the mechanical elevation lens (i.e., this is best-case detection); for *B1* and *B2* we used the left- and right-hand matrix apertures to incoherently spatially compound in elevation, bringing out the small scatterers, while in *C1* and *C2* the elevation beam formation was coherent. In each case the image dynamic range was adjusted to maximize the conspicuity of the micro-calcifications. While the simulation was of a volume, only elevation slices are shown for clarity—the azimuth apertures of each array are the same. The results are intriguing. While *B1* shows an expected improvement over *A1* and promise in detecting the *free-standing* micro-calcifications, a continuous coherent receive aperture is superior when a specular structure is nearby (compare *B2* to *C2*).

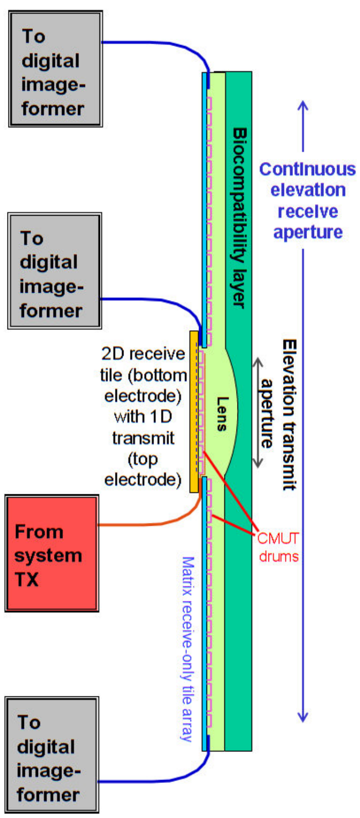

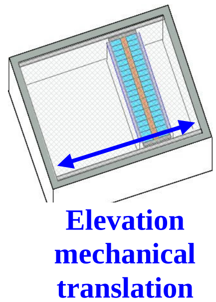

Figure 7: breast volumetric scanner: translation (above) and elevation view (left). The "C" configuration with 1D cMUT TX and continuous 2D RX is depicted. This 1D/2D combination is possible because of flexibility in the cMUT's manufacturing process.

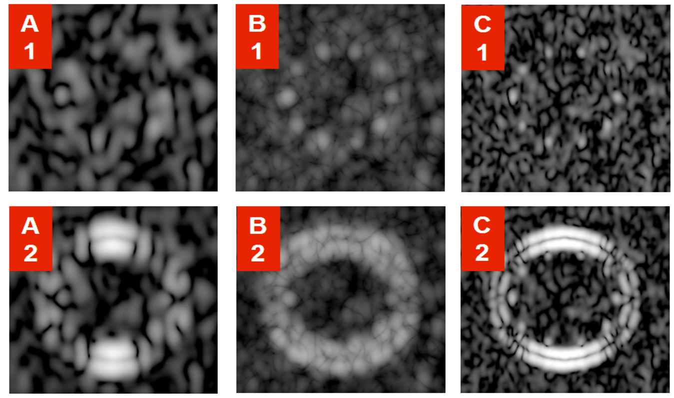

Figure 8: Elevation-plane images from automated breast scanner designs: "A" = 1D array; "B" = PZT 1D transmit, matrix receive on two apertures abutting the transmitter; "C" = cMUT 1D transmit allowing for a continuous 2D receive aperture and fully coherent RX processing.

C. Reconfigurable arrays

Reconfigurable arrays are an attractive method for dealing with matrix apertures with far more elements than the system or the probe-to-system interconnect can handle. Elements whose delay values are equal (or nearly so) in a given beam are wired together at the transducer, so that the system needs to supply a much smaller number of independent transmit signals and receive delay profiles. We review published work and then consider a new approach.

GE and Stanford [18] have made reconfigurable annular arrays generated from a matrix of cMUTs, and a switching ASIC for portable applications. The objective was to cut down on the channel count at the system. A 20-ring static cMUT array was initially scanned by mechanical translation. On the IC side, a 16x16 matrix of switches with 1024 elements was connected to a 16x16 PZT array, demonstrating aperture translation. This array concept was continued in [19], grouping sub-elements along iso-phase lines. Development of the interconnect involved choosing an interposer substrate to support both the switch ASICs and flip-chip attach of the MEMS die. Further work [20] showed how to improve beam formation by adding an axicon section to a ring array.

Our group at Siemens has investigated ways to limit effects of parasitic resistance and capacitance in the switch-matrix. In the design of Figure 9, sized for transesophageal (TEE) imaging, we form an approximately circular, 10-mm diameter aperture from seven hexagonal structures containing a matrix of elements.

Given currently available high-voltage switch technology, a simple approach where chains of elements are wired up to create the required aperture will not work. Either the "off" capacitance of the switches is too high, or their "on" resistance is too high. This causes a highly undesirable apodization from the point where an electrical connection is made to the elements to the end of the chain. If the elements are made large enough to avoid these problems, the beam formation is badly degraded—the maximum steering angle is insufficient and sidelobe energy is created because of spatial aliasing.

Solutions to these issues were prompted by the lithographic ease and precision with which cMUTs can be overlaid on the switching circuit. It is convenient for the integrated circuit to be formed from regularly-shaped cells, but the cMUT elements are randomly overlaid. This spreads the unwanted acoustic sidelobe energy over a large angular range, which is more clinically acceptable than having "spikes" in the point spread function at specific angles. We also used a technique somewhat analogous to the anti-aliasing algorithms in LCD computer displays [21] to minimize the undesirable field characteristics caused by "jaggies" in the aperture. For a given steering angle it would be ideal for the lines of constant phase to be geometrically smooth; but this is not possible with finitely-sized elements. Anti-aliasing can be achieved by using two types of switch termed "trunk" and "spoke" switches. The spoke switches are smaller (and consequently higher-resistance) than the trunk switches. The trunk switches wire up electronic nodes to create a 1D array rotated to the desired beam angle. Spoke switches connect the (relatively coarsely-spaced) electronic nodes to the randomly-spaced

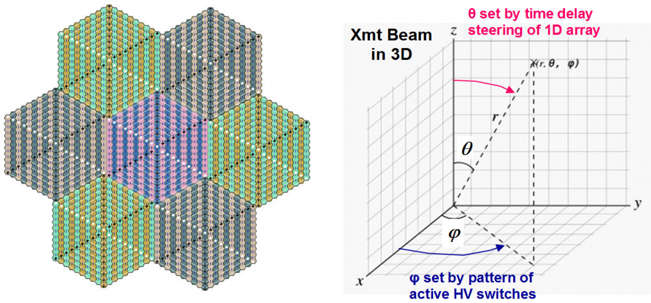

Figure 9: A cMUT reconfigurable array which presents a traditional 1D transmit-receive interface to the system and uses the imager to steer and focus in θ. A semiconductor switch-matrix creates the orthogonal scan dimension, φ.

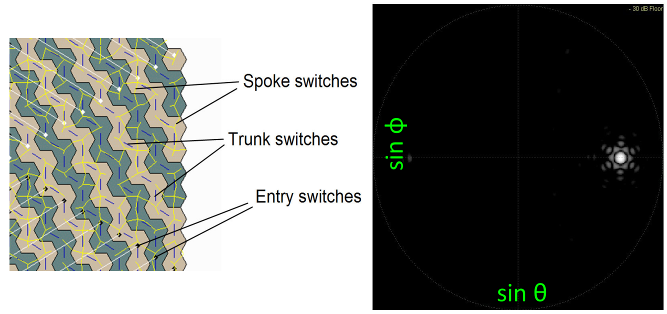

Figure 10: The left-hand image shows how a given φ is created by an arrangement of trunk and spoke switches. On the right, a 30 dB dynamic range plot illustrates the quality of focus created by the anti-aliased array.

array of acoustic elements overlaid on the electronics. The average pitch of the acoustic elements is significantly smaller than the electronic node pitch. The presence of the small spoke switches allows energy to be routed to the finely-sampled acoustic plane, while maintaining a feasible number of interconnects.

Our design with a 10 mm aperture and 4.5 MHz center frequency had around 1800 electronic nodes, and 3400 acoustic cells for enhanced beam formation. But it only required slightly more than 100 interconnects to the system because of the anti-aliasing scheme. Figure 9 shows the array's electronic configuration and its scanning geometry. The system beamformer defines the azimuth steering direction, while the elevation steering is set by the angle of the constant-phase lines created by the switch pattern.

The different types of switch are clarified in Figure 10. The electrical connections from the system to the switch-matrix are made at the "entry switches" shown in the left panel of the figure. The trunk and spoke switches are also indicated. The right panel shows a 1-way beam profile spanning ± 90° in azimuth and elevation with 30 dB white-to-black contrast. A clean steered focus with minimal sidelobe energy is evident.

VI. Review of Unique Signal Processing Requirements

A. *Defining element locations*

The Duke University group [22] has shown how to create a focus from a 96-element therapy array whose element locations and orientations are unknown. A least-squares triangulation approach was followed by an alignment to pressure amplitudes from simulation. This accounts for element size, and also crosstalk to some extent. Li [23] considered adaptive conformable arrays, devising an algorithm to deal both with acoustic path aberrations and uncertainty in element locations.

B. *Compensating for blocked acoustic paths*

Two types of blocked acoustic paths cause trouble in conformable arrays. Occlusion is the situation where beam formation has occurred adequately, but highly reflective structures cause shadowing or a complete lack of data beyond them. Wein *et al.* [24] dealt with this in the context of integrating ultrasound data into CT scans, a clinical strategy which has value in certain cancer treatments due to ultrasound's better depiction of structures such as lymph nodes. Volume data in their proposed workflow is acquired by a free-hand sweep without reorienting the probe in response to what is seen on the screen. The data are thus occluded in the same way as in a conformable array. Occlusion detection in this work was not fully automatic; it requires the operator to select a brightness value on the screen (see Figure 11). Beam lines are accepted into the data-set from the probe surface until (in the case of an occluded beam) a depth is found where the axial brightness variance drops below the empirical value. The data from occluded locations is removed from the set used to construct the final volume and replaced by data from other tiles. With adequate volume overlap, this operation does not threaten the integrity of the overall scan.

Cases where particles or air bubbles block elements in the near field, or where strong tissue reverberations cause an element's echo signals to be severely corrupted present more difficult issues, since the beam formation is damaged.

Li and O'Donnell [25, 26] devised ways to restore image quality degraded when elements are blocked or receiving strong reverberations. These can be *detected* simply by looking at the receive amplitude. To *compensate* for these lost elements, multiple receive beams are computed at each transmit angle and receive range to estimate the lateral source distribution. Target locations were estimated in the field, and cross-beam filtering could then reduce sidelobes. This approach works only works for point targets, so for in-vivo image improvement some image segmentation would be necessary.

C. Data Acquisition Speed

A typical radiology transducer in today's ultrasound systems produces 10 slices per second with between 100-200 beams per slice. A conformable array needs to create *volumes* of data rather than *slices*, so the beam count is squared. Also, the lateral extent of the scan required for, e.g., a complete liver is more than in a traditional use-case. Thus standard scan sequences using techniques such as sequential focus to approximate confocal imaging are several orders of magnitude too slow for our present purpose. Since diagnostically useful resolution and penetration must also be maintained, a radical approach is needed for a practical system. A detailed design of the scan is beyond the scope of this paper, so this section covers published work on foundations, and sketches a possible solution.

Hoctor and Kassam [27] noted that the imaging performance of a transmit-receive system is entirely determined by the co-array and its weighting function. The co-array, co-matrix or effective aperture (see also [28], which includes a review of beamforming research) is the lateral spatial frequency response at a given axial spatial frequency, and can be computed as the convolution of transmit and receive aperture functions. This result lends freedom to the acquisition process, since with a synthesized transmit aperture (STA) many interesting co-arrays can be found which cannot be created with a traditional delay-and-sum beamformer. The *k*-space framework [29] is very helpful as a means of gaining insight into STA imaging.

Before turning to aperture synthesis as a solution for conformable arrays, the goal of diagnostic utility must be reduced to an imaging criterion useful for judging different approaches. The information rate is a very useful way of quantifying imaging power. If the contrast-to-noise ratio is σ, the volume of the voxel is η, the scanned volume is V and the number of volumes scanned per second is R, then the information rate I is defined as $I \equiv \sigma^2 VR / \eta$, where I has units of inverse time. A flexible system can offer the end-user many trade-offs between the various parameters making up the information rate, but an increase in the information rate usually requires a wholesale redesign of the system. Sheer beamformer bandwidth—the ability to compute numerous parallel receive beams—is not sufficient to create the type of information rate needed for a real-time cardiac imaging [5], and certainly not for our case of a conformable array. Coherent processing of the output of the beamformer is equally critical. The information rate concept allows us to view a transducer as having an inherent information capability. The purpose of the scan and system design is to exhaust the transducer's information capacity, so that the limits on imaging are due to physics rather than instrumentation. Indeed, one way to view synthetic aperture scanning is as the construction of transmit and receive apertures with inexpensive geometries which combine into co-arrays with large information rates.

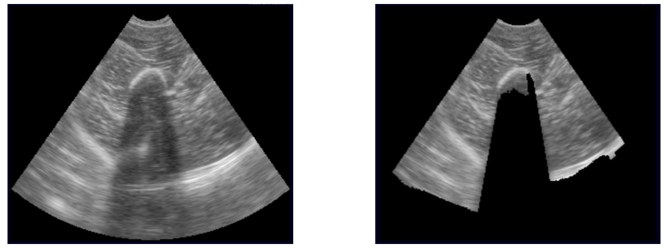

Figure 11: Occlusion detection in a slice. The data labeled as deeper than the occlusion are excluded from volume reconstruction (courtesy of W. Wein, White Lion Technologies AG).

The transmit-receive apodization ("T/R") matrix [30] is a helpful visualization of the co-array concept. For a 1D array of N elements, this matrix has dimensions NxN. Its rows correspond to transmit element positions, and its columns to receive element positions. The value in each element of the matrix is the outer product $M{=}a_T \cdot a_R^{\dagger}$ of the transmit a_T and receive a_R amplitude weightings († means vector transpose.) The co-array is a vector of length $2N\text{-}1$ formed from the cross-diagonal sum of the NxN matrix, and the far-field or near-focus beam profile is the Fourier transform of the co-array. The T/R matrix's rank is the number of transmit events necessary to scan a slice.

The power of transmit aperture synthesis can be seen from a scanning scheme where there are only two transmitters, located at the each end of the receive array. The T/R matrix shows that the resolution, if each transmitter is fired sequentially and the channel data stored for each transmit, is equal to that of a traditional approach at focus where the entire transmit aperture is used, as long as the receive apodization is set to the element-by-element product of the traditional transmit and receive apodization values. In fact, the resolution will exceed what is achieved in the traditional case since retrospective transmit focusing can be used on the synthetic aperture data to create a confocal system. The T/R matrix can also be used to predict that the SNR for this synthetic transmit aperture scheme is much worse than for traditional imaging.

This result generalizes to a 4-transmit scheme using a matrix transducer which produces a complete volume of data. While it is perhaps surprising that unfocused point transmitters might create resolution exceeding today's imaging performance, the achieved lateral bandwidth is what counts. For example, [31] shows that an out-of-focus converging beam has as much lateral bandwidth as achieved at its focus—in fact the lateral bandwidth from a Gaussian-apodized transducer is independent of depth before, during and after the geometric focus. One way to conceptualize an unfocused beam with high lateral bandwidth is to think of a constant-time slice as the wave propagates. Then the converging or diverging field is a spatial chirp created by the curvature of the wave-fronts, which is amenable to pulse compression signal processing. Bradley [32] illustrates that synthetic apertures created from several plane-wave transmit events are a good way of producing the critical angular diversity. Retrospective transmit focusing and coherent beam filtering to avoid beam group artifacts are presented in a cardiac application in that paper, but the results also hold for a conformable array.

Enormous volume rates are possible with these methods, but how can penetration be maintained at a competitive frequency? Chiao *et al.* [33] described how spatial coding can involve several beams' data in each transmit to increase the transmitted power and SNR. Using, e.g., a Hadamard matrix, data from spatially encoded transmit events can be linearly combined to recover "pure" STA firings with higher SNR. Transmit elements can also be grouped with appropriate delays to make virtual point-source (VPS) transmitters with the needed angular diversity and higher output power than can be achieved by a single element [34]. There are also opportunities [35] for temporal coding to further improve SNR. Any excess volume rate beyond what is demanded by the clinical application can be used for signal averaging or compounding. Tissue motion will set a upper limit on the number of firings which can be combined to create the volume. Increasing the number of transmit events creates redundant information in the data-set, making the imaging robust against real-life problems such as phase aberrations.

How, then, does one design the scanning for a conformable array? Briefly, the co-array must be continuous, to avoid Gibbs ripple in the point-spread functions, and it must create an optimal information rate. For simplicity, we will consider only 1D arrays, but the results easily generalize to volume imaging. Three simple building-blocks are the point source, the line source and the plane wave. To create the lateral spectra we can either take the Fourier transform of the field created by each type of source, or spatially scale and reverse the aperture function [29].

A point source located at $(x_0, 0)$ in the x-z plane has a point lateral spectrum located at $f_x = (x_0 / \lambda)\cdot(x_0^2 + z^2)^{-1/2}$, at a depth of z. A line source with width w extending from $(-w/2, 0)$ to $(w/2, 0)$ has a lateral spectrum which is a line with support extending a distance $f_x = (w / \lambda)\cdot(w^2 + 4z^2)^{-1/2}$, centered at the origin $f_x = 0$. The magnitude of the spectrum is the same as that of the source, but scaled to fit the line of support. Note that in both of these cases the lateral spectrum is a function of depth z. A plane wave has a depth-independent lateral spectrum, and for typical imaging situations a steered, unfocused transducer can be assumed to produce a largely plane wave throughout the region of interest. If the plane wave is steered at an angle θ_T, its field is:

$$\exp(j2\pi\,[\,ft - (x\cdot\sin\theta_T) / \lambda - (z\cdot\cos\theta_T) / \lambda\,]\,)$$

The lateral spectrum is obtained by Fourier transforming this field at a given frequency to give $\delta(f_x - \sin\theta_T / \lambda)$, a point lateral response which is not a function of location in the sound field. These simple considerations are enough to make interesting statements about the types of imaging possible.

As outlined in [27], the co-array is formed by convolving transmit and receive lateral spectra, and the point-spread function is the Fourier transform of the co-array. Following [35], if we position two point transmitters at the ends of a line receiver, the co-array becomes continuous, with twice the spatial-frequency extent of the receiver. The transmit-receive lateral bandwidth is then:

$$(a / \lambda)\,(a^2 + z^2)^{-1/2} = 2\cdot\sin[\tan^{-1}(a / 2z)] / \lambda$$

which is the maximum achievable for an aperture of size a.

However, this assumes that the elements have no directivity, so for a practical solution, the receive aperture needs to be limited to a constant F-number, growing as the beam moves deeper into the tissue. Once again, the transmitter choice is made by matching its lateral spectrum with what the receiver can produce. If the F-number $F_\#$ is kept constant, the lateral bandwidth of the receiver becomes independent of depth and has a region of support of $(F_\#\,\lambda)^{-1}$. Two plane waves will match the receiver if they are emitted from the transmitter at angles $\pm\,\theta_T$, where $\sin\theta_T = 0.5/F_\#$. At a certain depth, it will no longer be possible to maintain a constant F-number, so we can revert to the two point-source approach beyond that depth. In both of these cases, the image plane is acquired with only two firings. In the first, the two point sources are fired sequentially. With the plane-wave approach, we fire the positive and negative-angled waves in turn. Ustuner *et al.* [36] discusses the plane-wave or axicon approach in more detail, and suggest weakly diverging waves to match a convex probe geometry.

Diverging waves, such as made by the virtual point sources in [34], lose energy with depth, so a compromise needs to be made between the lateral bandwidth and SNR, controlled by location of the virtual point source. If the VPS location is a short distance behind the receive array, lateral bandwidth will be high but SNR is relatively low, and vice versa. Alternatively, the VPS can be positioned within the field, which follows from [31]. The interconnect and imaging system must be capable of sustaining an adequate volume rate to match the transducer and scan plan.

D. Volume registration and stitching

How should data volumes from multiple tiles be combined? This "stitching" problem divides into (1) an algorithm for volume alignment, and (2) means to measure the similarity of the overlapping parts of two volumes which have been registered. The group at Siemens Corporate Research [37] used a variational approach to compute deformable registration by directly computing the displacement field.

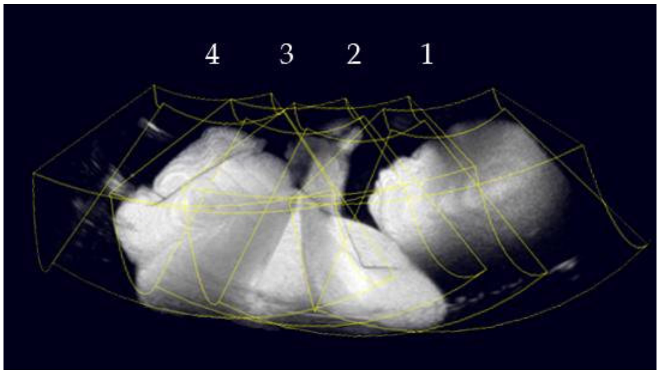

Figure 12: A large-volume data set created by aligning and stitching four acquisitions from a fetal phantom (courtesy of W. Wein.)

Wachinger *et al.* [3] discuss both stitching and similarity methods. Difficulties with alignment include compromises between pair-wise registration, which is computationally efficient but suffers from error accumulation, and simultaneous registration of all volumes, which is ideal but computationally costly. The presence of speckle in ultrasound images complicates the similarity measures: popular measures such as sums of squared differences, normalized cross-correlation, correlation-ratio and mutual information do not work well in the presence of speckle. Instead, the authors placed ultrasound-specific similarity measures based on noise models using Rayleigh statistics in a maximum-likelihood estimation framework. Overall, the ultrasound volume stitching problem appears tractable, especially when implemented on graphics processors (GPUs). Figure 12 shows an example of these algorithms applied to a fetal phantom.

E. Aberration correction

The aperture size achievable in a conformable array will be limited by phase aberration as well as motion. In [38] the phase aberration was estimated using correlation of channel signals with the beam-sum. This approach avoids the problem of a single bad estimate propagating to every subsequent element in the array. Channel correlation sums are filtered in range before conversion to element time estimates. Their small in-vivo study data showed 27 ns standard deviation of abdominal aberration, with 100 ns maxima in healthy volunteers. Beam quality for today's apertures is impacted when aberration exceeds 5-10% of a period. Larger conformable apertures are likely to be more sensitive to aberration, and the patient population has more sound-speed variation than normal subjects due to its demographics.

Li and O'Donnell [39] considered a flexible array finely sampled in azimuth but coarsely sampled in elevation. Mechanical movement of a 1D array emulated a conformable transducer. The authors simultaneously corrected for phase aberration in the phantom, as well as the shape of the conformable array.

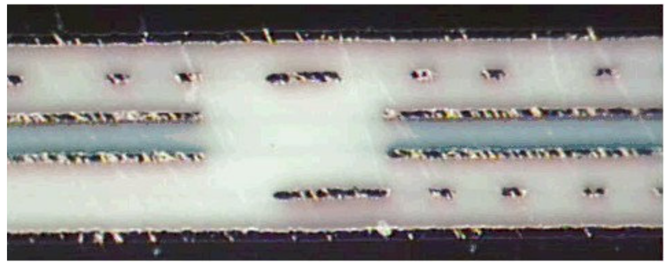

Figure 13: Cross-section of liquid-crystal polymer (LCP) substrate showing embedded flexible interconnect (courtesy of G. Thomas, Endicott Interconnect.)

Conclusions

In this paper we explained the motivation for conformable arrays, explored design requirements and postulated an idealized array design. After reviewing progress which has been made on hardware realizations, and discussing some new results on automated scanning and reconfigurable arrays, we considered the types of image formation and processing algorithms especially relevant to such transducers. Phase aberration and tissue movement place physical limitations on information rate improvements in the short and medium terms. We conclude by speculating on the types of development which would be needed to create a clinically useful device.

On the acquisition side, the front-end electronics [16] and beam formation [40] need to be located at the transducer element, while the cost and power of a channel must continue to shrink. Bandwidth to the system box and the availability of sufficient numerical processing power to handle the image formation and signal processing tasks outlined earlier complete the picture of requirements. Several trends in electronic manufacturing, such as 3D packaging and flexible interconnect (Figure 13 is an example of the latter) should make the difficult but worthwhile goal of large-volume, operator-independent ultrasound imaging reachable in the near future. All of the constituent technologies exist, so the task which remains is one of integration.

Acknowledgements

We thank the following people for support and for allowing reproduction of their work: Paul Wagner, Pierre Khuri-Yakub, Aaron Dann, Glen Thomas, Igal Ladabaum, Klaus Hambüchen, Wolfgang Wein and Haim Shafir.

References

[1] B. S. Garra, "Radiology must change to retain ultrasound role," *Diagnostic Imaging*, vol. 27, pp. 27-32, 2005.

[2] R. J. Littlefield, *et al.*, "MUSTPAC 3-D ultrasound telemedicine/telepresence system," in *IEEE Ultrasonics Symposium*, 1998, pp. 1669-1675 vol.2.

[3] C. Wachinger, *et al.*, "Registration Strategies and Similarity Measures for Three-dimensional Ultrasound Mosaicing," *Academic Radiology*, vol. 15, pp. 1404-1415, 2008.

[4] R. S. C. Cobbold, *Foundations of biomedical ultrasound*. New York: Oxford University Press, 2007.

[5] K. Ustuner. (2008, accessed Aug. 31, 2010). High Information Rate Volumetric Ultrasound Imaging. Available: www.medical.siemens.com/siemens/sv_SE/gg_us_FBAs/files/misc_downloads/Whitepaper_Ustuner.pdf

[6] C. Daft, *et al.*, "Microfabricated ultrasonic transducers monolithically integrated with high voltage electronics," in *IEEE Ultrasonics Symposium*, 2004, pp. 493-496 Vol.1.

[7] I. Ladabaum and S. H. Maslak, "Microfabricated ultrasonic transducers with curvature and method for making the same," US Patent 7,779,531, Aug. 24, 2010, 2010.

[8] K. A. Wong, *et al.*, "Curved micromachined ultrasonic transducers," in *IEEE Ultrasonics Symposium*, 2003, pp. 572-576 Vol.1.

[9] D. Kumar, *Six Sigma Best Practices: A Guide to Business Process Excellence for Diverse Industries*. Fort Lauderdale, FL: J. Ross, 2006.

[10] A. E. Dann, *et al.*, "Fabrication of a conformal ring-annular ultrasound array," in *Medical Imaging 2010: Ultrasonic Imaging, Tomography, and Therapy*, San Diego, California, USA, 2010, pp. 76290R-8.

[11] D. B. Bennett, *et al.*, "A conformal ultrasound transducer array featuring microfabricated polyimide joints," in *Health Monitoring of Structural and Biological Systems 2009*, San Diego, CA, USA, 2009, pp. 72951W-8.

[12] R. S. Singh, *et al.*, "Simulation, Fabrication, and Characterization of a Novel Flexible, Conformal Ultrasound Transducer Array," in *IEEE Ultrasonics Symposium*, 2007, pp. 1824-1827.

[13] D. J. Powell and G. Hayward, "Flexible ultrasonic transducer arrays for nondestructive evaluation applications. II. Performance assessment of different array configurations," *Ultrasonics, Ferroelectrics and Frequency Control, IEEE Transactions on*, vol. 43, pp. 393-402, 1996.

[14] X. Zhuang, *et al.*, "Flexible transducer arrays with through-wafer electrical interconnects based on trench refilling with PDMS," in *IEEE 20th International Conference on Micro Electro Mechanical Systems*, 2007, pp. 73-76.

[15] D. Kirbach and T. A. Whittingham, "3D ultrasound—the Kretztechnik Voluson approach," *Europ. J. Ultrasound* vol. 1, pp. 85-89, 1994.

[16] C. Daft, *et al.*, "A Matrix Transducer Design with Improved Image Quality and Acquisition Rate," in *IEEE Ultrasonics Symposium*, 2007, pp. 411-415.

[17] B. E. Hashimoto, "Sonographic assessment of breast calcifications," *Curr. Probl. Diagn. Radiol.*, vol. 35, pp. 213-8, Nov-Dec 2006.

[18] R. Fisher, *et al.*, "Reconfigurable arrays for portable ultrasound," in *IEEE Ultrasonics Symposium*, 2005, pp. 495-499.

[19] R. Wodnicki, *et al.*, "Multi-row linear cMUT array using cMUTs and multiplexing electronics," in *IEEE Ultrasonics Symposium*, 2009, pp. 2696-2699.

[20] H. Fong, *et al.*, "Hybrid beamforming and steering with reconfigurable arrays," *Ultrasonics, Ferroelectrics and Frequency Control, IEEE Transactions on*, vol. 57, pp. 1311-1319, 2010.

[21] J. C. Platt, "Optimal filtering for patterned displays," *Signal Processing Letters, IEEE*, vol. 7, pp. 179-181, 2000.

[22] R. J. McGough, *et al.*, "Shape calibration of a conformal ultrasound therapy array," *Ultrasonics, Ferroelectrics and Frequency Control, IEEE Transactions on*, vol. 48, pp. 494-505, 2001.

[23] P.-C. Li, *et al.*, "Adaptive ultrasound imaging systems using large, two-dimensional, conformal arrays," in *IEEE Ultrasonics Symposium*, 1994, pp. 1625-1628 vol.3.

[24] W. Wein, *et al.*, "Integrating Diagnostic B-Mode Ultrasonography Into CT-Based Radiation Treatment Planning," *Medical Imaging, IEEE Transactions on*, vol. 26, pp. 866-879, 2007.

[25] P. C. Li, *et al.*, "Blocked element compensation in phased array imaging," *Ultrasonics, Ferroelectrics and Frequency Control, IEEE Transactions on*, vol. 40, pp. 283-292, 1993.

[26] P. C. Li and M. O'Donnell, "Efficient Two-Dimensional Blocked Element Compensation," *Ultrasonic Imaging*, vol. 16, pp. 164-175, 1994.

[27] R. T. Hoctor and S. A. Kassam, "The unifying role of the coarray in aperture synthesis for coherent and incoherent imaging," *Proceedings of the IEEE*, vol. 78, pp. 735-752, 1990.

[28] J. A. Johnson, *et al.*, "Coherent-array imaging using phased subarrays. Part I: basic principles," *Ultrasonics, Ferroelectrics and Frequency Control, IEEE Transactions on*, vol. 52, pp. 37-50, 2005.

[29] W. F. Walker and G. E. Trahey, "The application of k-space in pulse echo ultrasound," *Ultrasonics, Ferroelectrics and Frequency Control, IEEE Transactions on*, vol. 45, pp. 541-558, 1998.

[30] R. Y. Chiao and L. J. Thomas, "Aperture formation on reduced-channel arrays using the transmit-receive apodization matrix," in *IEEE Ultrasonics Symposium*, 1996, pp. 1567-1571 vol.2.

[31] R. Zemp and M. F. Insana, "Imaging with unfocused regions of focused ultrasound beams," *Journal of the Acoustical Society of America*, vol. 121, pp. 1491-1498, 2007.

[32] C. Bradley. (2008, accessed Aug. 31, 2010). Retrospective Transmit Beamformation. Available: www.medical.siemens.com/siemens/sv_SE/gg_us_FBAs/files/misc_downloads/Whitepaper_Bradley.pdf

[33] R. Y. Chiao, *et al.*, "Sparse array imaging with spatially-encoded transmits," in *IEEE Ultrasonics Symposium*, 1997, pp. 1679-1682 vol.2.

[34] S. Nikolov and J. A. Jensen, "Virtual ultrasound sources in high-resolution ultrasound imaging," in *Medical Imaging 2002: Ultrasonic Imaging and Signal Processing*, San Diego, CA, USA, 2002, pp. 395-405.

[35] T. X. Misaridis and J. A. Jensen, "An effective coded excitation scheme based on a predistorted FM signal and an optimized digital filter," in *IEEE Ultrasonics Symposium*, 1999, pp. 1589-1593 vol.2.

[36] K. F. Ustuner, *et al.*, "Pulse-echo beamformer with high lateral and temporal resolution and depth-independent lateral response," in *IEEE Ultrasonics Symposium*, 2001, pp. 1559-1564 vol.2.

[37] D. Zikic, *et al.*, "Fast Deformable Registration of 3D-Ultrasound Data Using a Variational Approach," in *Medical Image Computing and Computer-Assisted Intervention – MICCAI 2006*. vol. 4190, R. Larsen, *et al.*, Eds.: Springer Berlin / Heidelberg, 2006, pp. 915-923.

[38] K. W. Rigby, *et al.*, "Improved in vivo abdominal image quality using real-time estimation and correction of wavefront arrival time errors," in *IEEE Ultrasonics Symposium*, 2000, pp. 1645-1653 vol.2.

[39] P.-C. Li and M. O'Donnell, "Phase aberration correction on two-dimensional conformal arrays," *Ultrasonics, Ferroelectrics and Frequency Control, IEEE Transactions on*, vol. 42, pp. 73-82, 1995.

[40] D. Liu, *et al.*, "Sigma-delta dynamic receive beamforming," in *IEEE Ultrasonics Symposium*, 2008, pp. 1270-1273.